Optical, Electronic, and Structural Properties of Uncoupled and Close-Packed Arrays of InP Quantum Dots

Olga I. Micić,* Kim M. Jones, Andrew Cahill, and Arthur J. Nozik*

National Renewable Energy Laboratory, 1617 Cole Boulevard, Golden, Colorado 80401

Received: March 31, 1998; In Final Form: August 10, 1998

Solid films consisting of close-packed arrays of InP quantum dots have been prepared by slowly evaporating colloidal solutions of InP quantum dots. The diameters of the quantum dots were controlled to be between about 30 to 60 Å; size-selective precipitation yielded a size distribution of about 10% about the mean diameter. The arrays show regions of hexagonal order, as well as disordered regions. Oxide layers can form irreversibly on the quantum dot surface and limit the effectiveness of the size-selective precipitation. Photoluminescence spectra obtained from close-packed films of InP quantum dots formed from quantum dots with a single mean diameter and from a mixture of two quantum dot sizes show that energy transfer occurs from the photoexcited smaller quantum dots to the larger quantum dots. The efficiency of this energy transfer process is high.

I. Introduction

The creation and study of arrays of metal[1−6] and semiconductor[7−21] quantum dots (QDs) are topics of great current interest. Semiconductor QD arrays can be formed either from colloidal nanocrystals[7−12] or via self-organization of nanostructures grown from the vapor phase by epitaxial deposition.[15−21] QD arrays show very interesting optical and electronic properties including reversible tuning of metal−insulator transitions,[22] enhanced nonlinear optical effects,[23] photoinduced energy transfer processes,[24,25] Coulomb blockade effects,[26] lasing action,[27,28] nonequilibrium carrier transport,[29] and resonant tunneling.[30]

Recent advances have been made in the synthesis of well-crystallized and passivated InP QDs that exhibit very high quantum yields for band-edge emission;[31−35] these experiments, together with advances in the theoretical analyses of their electronic structure, have established the optical properties and electronic states of InP QDs as a function of size.[36−39]

The synthesis of close-packed arrays of InP QDs is of interest in order to explore cooperative phenomena, such as interdot electronic coupling, energy transfer, and collective excitation. In close-packed arrays of QDs, the excitonic state is not localized within a single quantum dot, but can be delocalized through the dot array via energy transfer arising from dipole−dipole interactions.[23−25,40−42] Optical and electronic characterization of QD arrays in the form of solid-state materials is important for understanding collective phenomena. Optimal manifestation of these properties depends on the QD quality, which includes uniformity of size, shape, and morphology, and crystal perfection, surface passivation, and spatial orientation. Recent literature has reported success in forming close-packed QD arrays in three-dimensional superlattices, as well as in sheet structures containing one or more layers of QDs; this work includes metal nanoparticles (i.e., Au and Ag[1−6,22,43−45]), and semiconductor nanocrystals (ZnO,[9] Fe_2O_3,[7] CdS,[10] CdSe,[14,11] AgS,[12] ZnSe,[46] SiGe,[47] InAs,[48] InGaAs,[49] and Ge[50]).

Our previous studies were aimed at understanding the properties of uncoupled QDs.[33−36] In this work we report on improvements in the quality of synthesized uncoupled colloidal InP QDs, as well as our studies of coupled InP QDs in the form of self-assembled arrays.

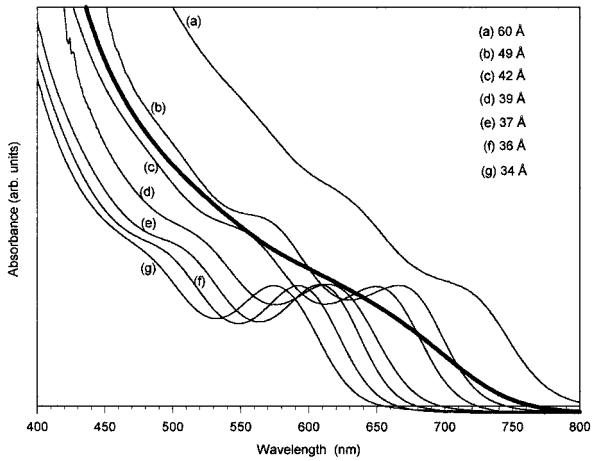

Figure 1. Absorption spectra of InP QDs after the initial colloidal preparation (bold line) and after size selective precipitation (spectra are for QD sizes ranging from 26 to 60 Å).

II. Experimental Section

A. Synthesis of Colloidal InP QDs. Colloidal InP QDs were synthesized by colloidal chemistry methods using an indium salt (either $In(C_2O_4)_3$, InF_3, or $InCl_3$) and tris-(trimethylsilyl)phosphine ($P(SiMe_3)_3$) as starting reactants; the reactants are heated for 3 days at 260−280° C in the presence of trioctylphosphine oxide (TOPO) and trioctylphosphine (TOP). The synthesis is conducted in rigorously air-free and water-free atmospheres; during the synthesis the QDs are capped with TOPO/TOP, which produce a compact hydrophobic shell on the particle surface. Details of the preparation are given in refs 33 and 34. Fractionation of the QD particles into different sizes was achieved through the selective precipitation method described by Murray and co-workers.[51] As an illustration, Figure 1 shows the absorption spectra of colloidal InP QDs initially prepared (bold line) and after fractionation by size-selective precipitation. The initial colloidal solution shows a structureless

10.1021/jp981703u CCC: $15.00
Published on Web 09/26/1998

absorption spectrum with a size distribution of about 30%. After size-selective precipitation, the samples have a size distribution of about 10−13%. However, we note that the size selective method is only effective for unoxidized InP QDs.

The resulting InP QDs contain a capping layer of TOPO, which can be readily substituted by several other types of capping agents, such as thiols, furan, pyridines, amines, fatty acids, sulfonic acids, and polymers. Finally, the QDs can be studied in the form of colloidal solutions or close-packed films.

B. Etching of Colloidal InP Quantum Dots with HF. Intense band-edge emission from InP QDs can be achieved after etching the particles with a dilute alcoholic solution of HF.[35] Our previous procedure for etching InP QDs followed from the work of Waldeck and co-workers,[52] where HF was used to remove the surface native oxide from single-crystal InP. We improved the etching procedure by using two liquid phases during the etch. The two-phase system was formed by mixing 1−10 μL of a butanol solution containing 5% HF and 10% H_2O, with 4 mL of a colloidal solution containing hexane, butanol, and acetonitrile (1:0.1:1), 2−5% TOPO, and the InP QDs (particle concentration 4×10^{-6} M). The QDs are dispersed in the lower density nonpolar hexane phase, while the HF, butanol, and H_2O remain in the acetonitrile phase. This ensures that the etching rate is slow and uniform. The mixture is shaken, left overnight, and then the hexane phase containing the QDs is separated and used. For fresh colloidal InP QD solutions, lower concentrations of HF are required than for solutions that were exposed to air or stored for long periods of time. Throughout the etching process, Teflon or polyethylene vessels, syringes, and tubes were used.

Freshly prepared solutions give the best emission quantum yields, and after etching the adsorption spectra show only a slight shift to the UV (20 nm for 26-D dots) and a slight loss of intensity of the exciton peak. In air the QDs very slowly (weeks) lose emission intensity, while in an air-free atmosphere the emission does not change for months. The quantum yield of band-edge emission before etching is less than 1%, and after etching it ranged from 5 to 40% at room temperature. At 4 K the quantum yield was 60%.

C. Preparation of Close-packed Films. The volume and the concentration of an aliquot of InP colloidal solution are adjusted to control whether a dense monolayer or multilayers of QDs are formed upon evaporation. Following Murray,[14] optically thin, transparent (nonscattering), and close-packed QD films were formed by slow evaporation of the QD solution in a mixture of hexane and octane (0.9:0.1) on sapphire plates. All close-packed QD films contained InP QDs that had been treated with HF to improve PL emission. All measurements were collected from thin films with a thickness of about 0.25 μm to minimize reabsorption of emitted photons.

D. Optical Characterization. Optical absorption spectra were collected at room temperature using a Cary 5E UV−Vis−NIR spectrophotometer. Photoluminescence spectra were obtained at room temperature using a SPEX Fluorolog-2 spectrometer. The absorbance of thin films was always less than 0.1 at the peak of the first excited state in order to minimize reabsorption of emitted photons. In mixed solids, smaller dots have an absorbance of 0.05 at the peak of the first excited state. Luminescence quantum yields for QD solids and solutions were measured relative to the known luminescence intensities of organic dyes.

E. Transmission Electron Microscopy. A Phillips CM-30 electron microscope operating at 200 kV was used for transmission electron microscopy (TEM). Imaging was carried out in bright field with an objective aperture selected to permit lattice imaging of the ⟨111⟩ zinc blende plane. The samples were prepared by placing 2.5 μL of a dispersion of QDs in a mixture of octane(0.9)/octanol(0.1) directly onto a copper grid supporting a thin film of amorphous carbon and allowing it to slowly evaporate.

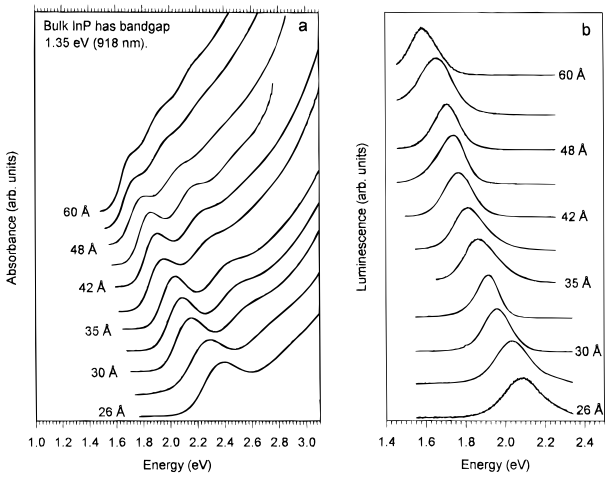

Figure 2. Absorption and emission spectra of InP QDs as a function of a diameter.

III. Results and Discussion

A. Optical and Structural Characterization of InP QDs. Figure 2a shows the absorption spectra of InP QDs obtained after selective precipitation methods were used for different initial colloidal solutions; the QD diameters range from 25 to 60 Å. The absorption spectra show one or more broad excitonic peaks, which reflect substantial inhomogeneous line broadening arising from the QD size distribution; as expected, the spectra shift to higher energy as the QD size decreases. Higher energy transitions above the first excitonic peak in the absorption spectra can also be seen. The spread in QD diameters is generally about 10%. All of our QD preparations are in the strong confinement regime since the Bohr radius of bulk InP is about 100 Å. Etching of InP QDs with HF suppresses the red-shifted emission from deep surface traps by passivating P vacancies and trap states on the nanocrystallite surface; this produces emission that is dominated by radiative recombination from the band edge. Figure 2b shows the room-temperature photoluminescence spectra as a function of QD particle size after etching the QDs with HF.

A major characteristic of InP QDs is that the surface oxidizes easily upon exposure to air, and a surface oxide layer is formed; this was confirmed by Guzelian and co-workers[32] using X-ray photoelectron spectroscopy. This also occurs with bulk InP. The TOPO/TOP stabilizer on the QD surface does not prevent surface oxidation. We also confirmed by NMR that our InP QD samples oxidized during exposure to air.[53]

With an oxide layer present, the optical absorption of InP QDs shows little structure, and excitonic transitions become less pronounced. The oxide layer also limits the effectiveness of the size-selective precipitation. Furthermore, it is known that the oxide layer suppresses charge carrier recombination and corrosion, and gives InP its unique photoelectrochemical properties, especially enhanced stability.[53,54] Although surface oxidation enhances the stability of bulk InP, easy oxidation of InP QDs creates problems for the study of quantization effects since these effects are very sensitive to the core InP QD size, shape,

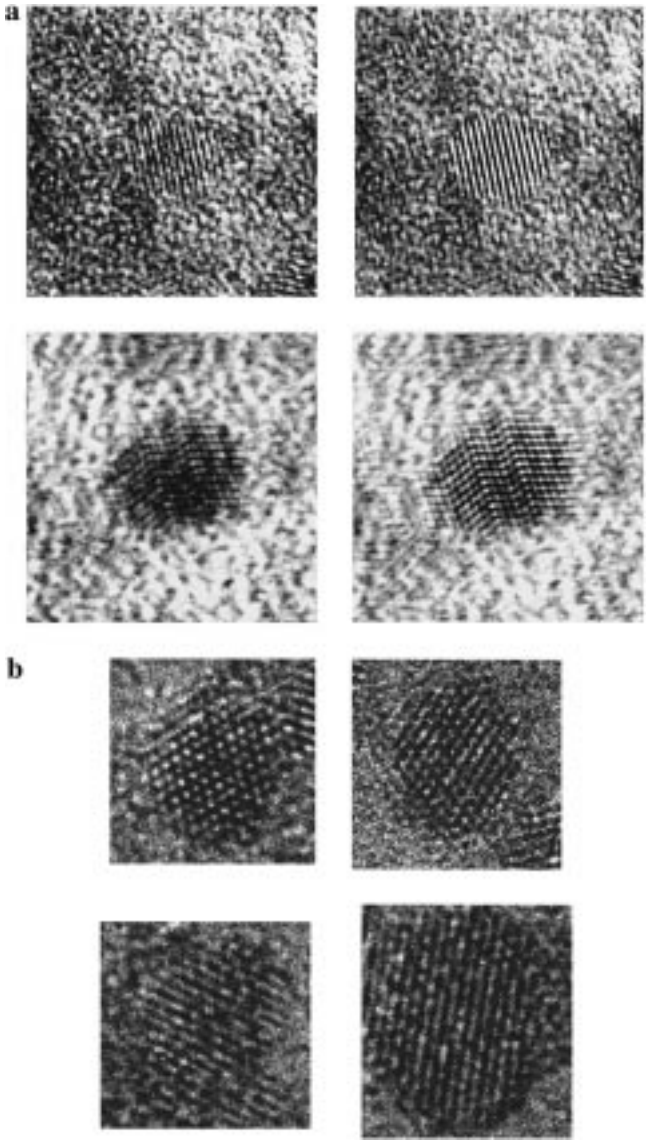

Figure 3. (a) TEM of 60-Å-diameter InP QDs oriented with the ⟨111⟩ axis in the plane of the micrograph, bottom figs show existence of stacking faults, (b) HRTEM of 44−65 Å InP QDs showing elliptical shape and facets.

and core−shell structure. To avoid QD sample oxidation after synthesis, we fractionated the QDs by size in an air-free atmosphere.

InP QDs have a zinc blende InP structure.[33] High resolution TEM was used to determine the average size, shape, and size distribution. The best edge contrast was obtained with QDs that were etched with HF. Images of single InP QDs are seen in Figure 3. The InP QDs generally exhibit an elliptical shape. In Figure 3a, images on the left are the original images while those are the right are computer-enhanced. The columns of atoms display the characteristic cubic pattern of the ⟨111⟩ projection of the InP zinc blende crystal structure. Most of the QDs exhibit no faults; examples are shown in the upper images of Figure 3a viewed along the ⟨111⟩ direction. However, occasional nanocrystals do show defects as can be seen in the lower images of Figure 3a; the defects in this nanoparticle consist of three stacking faults (twin planes). Figure 3b shows high-resolution TEM images that exhibit elliptical QD shapes. Faceting can also be readily seen in these images, but the detailed geometrical shapes associated with these facets have not yet been established.

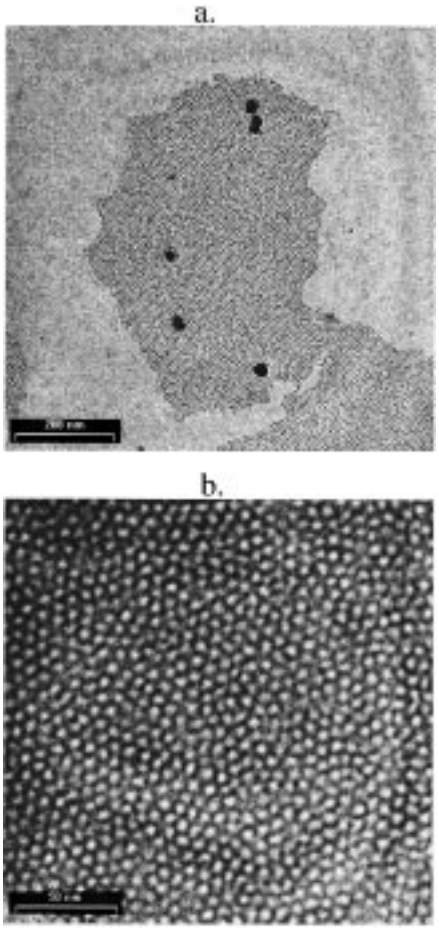

Figure 4. TEM of array of 57-Å-diameter InP QDs formed by slow evaporation of the QD colloidal solution: (a) QDs show a tendency to self-organize, (b) a monolayer showing short-range hexagonal close packing.

InP QDs are randomly oriented on the carbon grid. This is to be compared with CdSe QDs,[11,14] which possess large electrical dipole moments[55,56] and consequently show strong orientation on carbon films; InP QDs to within first-order approximation should not possess an electrical dipole moment.[57]

B. Close-Packed InP QD Solids. Arrays of close-packed InP QDs can be formed by slowly evaporating colloidal solutions of capped QDs that have been treated with HF. Upon evaporation, the QD volume fraction increases and interaction between the QDs develops. This leads to the formation of a self-organized QD film. Figure 4a shows TEM micrographs of a monolayer made with InP QDs, which have diameters of 49 Å, and in which each QD remains separated from its neighbors by the TOPO/TOP capping groups. Figure 4b shows an enlarged region from Figure 4a in which the local hexagonal order is evident. Figure 5a also shows the formation of a monolayer organized in a hexagonal network made with QDs 57 Å in diameter, which are capped with dodecanethiol; InP QDs capped with oleyamine can also form monolayers with short range hexagonal order. Our preparations have size distributions of about 10%; with such a size distribution we are able to prepare 2-D monolayer arrays with only local order; multilayers of QDs exhibit random order (see Figure 5b).

To form colloidal crystals with a high degree of order in the QD packing, the size distribution of the QD particles must have a mean deviation less than about 5%, uniform shape, and excellent orientation on the substrate. Murray and co-workers[11] fabricated highly ordered 3-D superlattices of CdSe QDs that

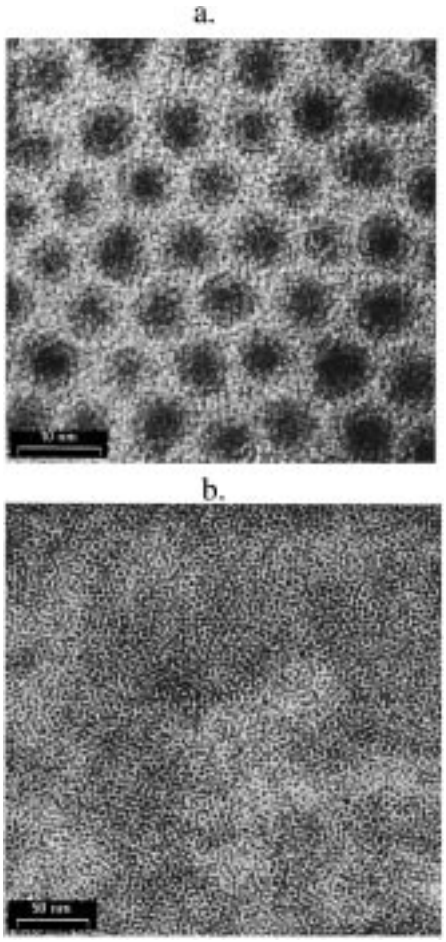

Figure 5. TEM of self-organized array of 49-Å-diameter InP QDs: (a) capped with dodecanethiol, and (b) multilayer, which is randomly oriented and formed from a pyridine colloidal solution.

have a size distribution of 3−4%. This novel QD configuration forms an ordered crystal lattice where QDs occupy the lattice sites analogous to atoms in a conventional crystal structure.

C. Energy Transfer by Excitons. Although three-dimensional QD superlattices have been fabricated, their electronic properties have not yet been sufficiently characterized because of the relatively small dimensions of the crystalline regions (5−50 μm). Energy transfer between QDs has also not been studied much because the quantum yield of band-edge emission was small and nonradiative recombination was high. However, long-range resonance transfer of electronic excitation in close-packed CdSe QD films has been observed by Kagan and co-workers.[24,25] In our experiments here we fabricated close-packed InP solids of QDs that were etched in HF; these multilayer films were optically transparent and the QDs were randomly ordered. In these solid films we also observed energy transfer from small QDs to large QDs. Figure 6 shows the emission spectra of a dilute QD solution and a close-packed film of QDs with diameters of 45 or 35 Å. The absorption spectra of uncoupled QDs in colloidal solution are virtually identical to those from a QD solid film formed from the solution. The absorption spectra for the two sizes are similar in shape, but blue shifted for the smaller QD size. For both sizes the peaks of the emission spectra of the close-packed films are red shifted with respect to the QD solution spectra. These observations suggest that energy transfer occurs within the inhomogeneous distribution of the QDs in the solid film. The observed red shift, together with a narrowing of the emission spectra, becomes more prominent for samples with a broadened size

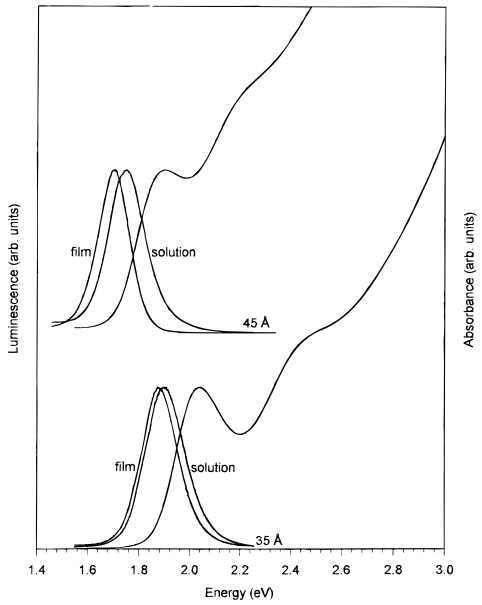

Figure 6. Absorption and luminescence spectra (λ_{exc} = 500 nm) of InP QDs in dilute colloidal solution and in close-packed films for 45- and 35-Å diameter QDs.

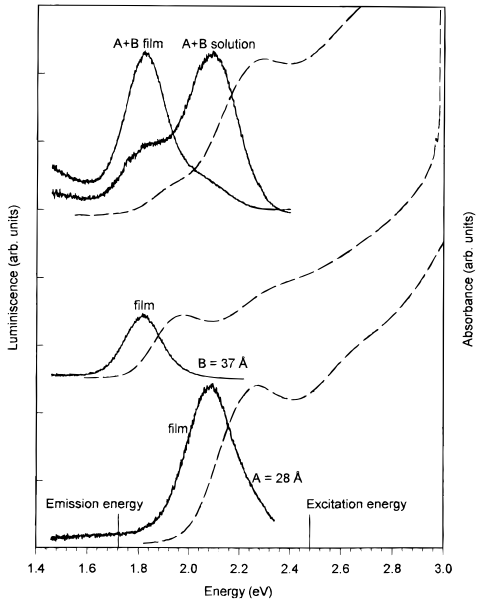

Figure 7. Absorption and luminescence spectra (λ_{exc} = 500 nm) of InP QDs with (a) two sizes (28 and 37 Å) in close-packed films prepared from a colloidal mixture of 28- and 37-Å-diameter QDs, (b) 37-D QDs only, (c) 28-D QDs only.

distribution; this is the case for the 45-Å InP QD sample (Figure 6), which has a broader size distribution (∼12%) compared to that for the 35-Å QD sample (∼8%).

We have also studied electronic energy transfer between close-packed QDs in a mixed system consisting of 20% larger dots (37 Å) and 80% smaller dots (28 Å). The absorption and emission spectra of the two QD samples with different sizes are presented in the bottom two plots in Figure 7 and are labeled A (donor) (28 Å) and B (acceptor) (37 Å). The absorption spectra (dashed lines) for the single-sized QD solution or the QD film are identical. The blue shifts in the absorption and emission spectra for the smaller QD size are as expected. The top of Figure 7 shows the absorption and emission spectra of the two QD sizes when they are mixed in solution and when mixed in the solid QD film. In the mixed QD solution, the

emission spectrum is the sum of the emission spectra of the two individual QD sizes; the absorption spectrum of the solution or the QD film is also the sum of the individual spectra. However, for the mixed QD film, the emission is primarily from the larger (37 Å) QDs; that is, emission from the small (28-D) QDs decreases and that from the 37-D QDs increases when the two sizes are mixed in the close-packed film. Photoluminescence excitation spectra also show that the emission from the large QDs originates from excitation of both small and large QDs. These results strongly indicate that energy transfer occurs from the higher energy states in the small QDs to the lower energy states in the large QDs.

Following Kagan and co-workers,[24,25] these experiments can be analyzed to yield information about the relative efficiency of energy transfer in the QD solid film. If we assume that energy transfer occurs via the dipole−dipole, Förster-type mechanism, then the distance R_0, at which the rate of energy transfer becomes equal to the rate of other mechanisms for nonradiative quenching of the excitation energy in the QD, can be estimated from

$$\frac{\varphi_{\mathrm{D,mixed}}}{\varphi_{\mathrm{D,pure}}} = 1 - \frac{\pi}{2}\gamma \exp\left(\frac{\pi\gamma^2}{4}\right)\mathrm{erf}\left(\frac{\pi^{1/2}\gamma}{2}\right) \qquad (1)$$

and

$$\gamma = C\left(\frac{4}{3}\pi R_0^3\right) \qquad (2)$$

where $n_{\mathrm{D,mixed}}$ = quantum yield of PL emission from small dots in a mixed QD film, $n_{\mathrm{D,pure}}$ = quantum yield of PL emission from QD film containing only small QDs, C = concentration (cm^{-3}), and erf = error function.

From Figure 7 we find that $n_{\mathrm{D,mixed}}/n_{\mathrm{D,pure}} = 0.8$. From our known concentration of 2.26×10^{17} InP molecules/cm^3 in the film, we calculate that $R_0 \approx 90$ Å; this is relatively high indicating efficient energy transfer. We note, however, that eqs 1 and 2 have been derived for energy transfer between uniformly dispersed and randomly oriented molecules. In our system the entity from which energy is being transferred is a QD with hundreds of InP molecules; therefore, it is not clear that eqs 1 and 2 can be properly applied to this system. If we use the QD particle concentration in the film instead of the total molecule concentration, this leads to an unrealistically high value for R_0 (700 Å).

To determine whether an R_0 of 90 Å (calculated from eqs 1 and 2 using the InP molecule concentration) is reasonable, we carried out a series of additional PL experiments to measure R_0 more directly. In these experiments an inert molecular diluent is added to the QD films to produce a known average separation between large (40 Å) and small (28 Å) QDs; the diluent was heptamethylnonane (HMN). A known amount of HMN was added to a hexane solution of the QDs, and the hexane was then evaporated to produce thin QD films containing the HMN. In all experiments the absorbance of the small and large QDs was 0.01 at the first excitation maxima. The distance (R) between the small (donor) and large (acceptor) QDs was varied by varying the HMN concentration; it could be calculated from the total QD volume and the HMN volume. The TOPO capping layer (11 Å) was also taken into account.

Figure 8 shows that when the separation between the QDs decreases from large values associated with high concentrations of the HMN diluent to small values in the close-packed film, the PL emission from the large QDs (acceptor) increases while the emission for the small QDs (donor) decreases. The emission

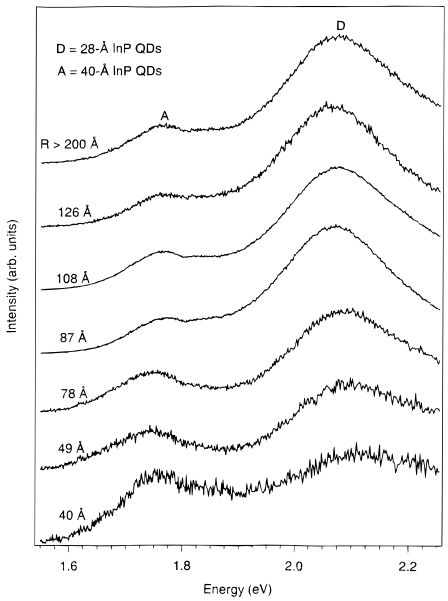

Figure 8. Luminescence of films of InP QDs with two sizes (28 and 40 Å) for different distance between QDs adjusted by the addition of heptamethylnonane.

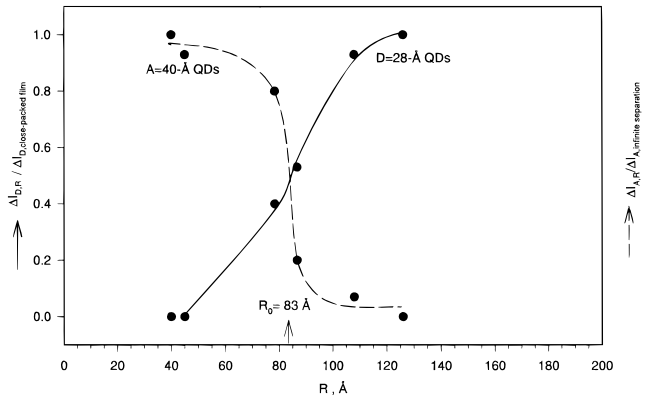

Figure 9. Change of the luminescence intensity in a film of 28- and 40-D InP QDs as a function of the separation between the QDs.

intensities for the small and large QDs do not change for $R >$ 108 Å in diluted films, and in close-packed films for $R <$ 49 Å with TOPO caps and $R <$ 40 Å with pyridine caps.

In Figure 9 we plot the R dependence of (1) the emission intensity of the 40-Å acceptor QDs (after subtracting the emission in the most diluted sample) divided by that of the acceptor QDs in the close-packed film, and (2) the emission intensity of the 28-Å donor QDs (after subtracting the emission of the close-packed film) divided by the intensity at high HMN dilution. The acceptor QD emission increases with decreasing R, and the donor emission decreases with decreasing R. Since R_0 is the separation distance at which the rate of energy transfer becomes equal to the rate of excitation energy quenching by other mechanisms, it can be estimated from Figure 9 by equating it to the R value at which 50% of the emission intensity of the donor is transferred to the acceptor (i.e., where the two curves cross). This yields $R_0 = 83$ Å, which is close to the value of 90 Å derived from eqs 1 and 2. However, further theoretical analysis of energy transfer between QDs is required to understand whether this apparent agreement is significant or coincidental.

Finally, we have preliminary results on photoconductivity in close-packed InP QD solids that show that the spectral response of the photocurrent follows the absorption spectra of QDs. The

I−V characteristics for the QD solids are nonlinear and have a threshold voltage; they are also independent of exciton energy and excitation intensity. Transport of carriers through the QD array is 3 orders of magnitude lower than that in InP QDs adsorbed on porous TiO_2 electrodes, where better charge separation on the InP/TiO_2 interface exists.[58]

D. Conclusion. Solid films of close-packed InP quantum dots were formed by slow, controlled evaporation of colloidal solutions of InP quantum dots. Narrow size distributions of the quantum dot colloidal solutions are required to achieve optimum packing and long-range order in the solid film. Size selective precipitation reduces the size distribution of the initially prepared colloidal dispersion to about 10%. This is sufficient to produce local hexagonal order in the close-packed quantum dot films, but not long-range order; a size distribution less than about 5% would be required for the latter. Irreversible oxidation of InP quantum dots limits the effectiveness of size selective precipitation. This is because a significant oxide layer on the quantum dot would decrease the actual size of the InP core compared to the nanocrystal size. Efficient long-range energy transfer from photoexcited small quantum dots to larger quantum dots in solid films of close-packed InP quantum dots was observed from photoluminescence experiments.

Acknowledgment. This work was supported by the U.S. Department of Energy, Office of Basic Energy Sciences, Division of Chemical Sciences. We are grateful to Dr. Chris Murray (IBM) for very helpful discussions on selective precipitation techniques and on formation monolayer array. We also thank Dr. Christian Kiesielowski (Lawrence Berkeley Laboratory) for obtaining the HRTEM images shown in Figure 3b.

References and Notes

(1) Harfenist, S. A.; Wang, Z. L.; Alvarez, M. M.; Vezmar, I.; Whetten, R. L. *J. Phys. Chem.* **1996**, *100*, 13904.

(2) Giersig, M.; Mulvaney, P. *J. Phys. Chem.* **1997**, *97*, 66334.

(3) Trau, M.; Saville, D. A.; Aksay, I. A. *Science* **1996**, *272*, 706.

(4) Brust, M.; Bethell, D.; Schiffrin, D. J.; Kiely, C. J. *Adv. Mater.* **1995**, *7*, 795.

(5) Heath, J. R.; Knobler, C. M.; Leff, D. V. *J. Phys. Chem. B.* **1997**, *101*, 189.

(6) Terrill, R. H.; Poslethwaite, T. A.; Chen, C.; Poon, C. D.; Terzis, A.; Chen, A.; Hutchison, J. E.; Clark, M. R.; Wignall, G.; Londono, J. D.; Superfine, R.; Falvo, M.; Johnson, C. S., Jr.; Samulski, E. T.; Murray, R. W. *J. Am. Chem. Soc.* **1995**, *117*, 12537.

(7) Bentzon, M. D.; van Wonterghem, J.; Morup, S.; Thölen, A. *Philos. Magn. B* **1989**, *60*, 169.

(8) Chang, S.; Liu, L.; Asher, S. A. *J. Am. Chem. Soc.* **1994**, *116*, 67.

(9) Spanhel, L.; Anderson, M. A. *J. Am. Chem. Soc.* **1991**, *113*, 2826.

(10) Vossemeyer, T.; Reck, G.; Katsikas, L.; Haupt, E. T. K.; Schulz, B.; Weller, H. *Science* **1995**, *267*, 1476.

(11) Murray, C. B.; Kagan, C. R.; Bawendi, M. G. *Science* **1995**, *270*, 1335.

(12) Motte, L.; Billoudet, F.; Lacaze, E.; Douin, J.; Pileni, M. P. *J. Phys. Chem. B.* **1997**, *101*, 138.

(13) Nozik, A. J.; Micic, O. I. *MRS Bull.* **1998**, *23*, 24.

(14) Murray, C. B. Synthesis and Characterization of II−VI Quantum Dots and Their Assembly into 3D Quantum Dot Superlattices. Ph.D. Thesis, Massachusetts Institute of Technology, 1995.

(15) Hanna, M. C.; Lu, Z. H.; Cahill, A. F.; Heben, M. J.; Nozik, A. J. *J. Cryst. Growth* **1997**, *174*, 605.

(16) Eaglesham, D. J.; Cerullo, M. *Phys. Rev. Lett.* **1990**, *64*, 1943.

(17) Snyder, C. W.; Orr, B. G.; Kessler, D.; Sander, L. M. *Phys. Rev. Lett.* **1991**, *66*, 3032.

(18) Wang, P. D.; Merz, J. L.; Medeiros-Ribeiro, G.; Fafard, S.; Petroff, P. M.; Akiyama, H.; Sakaki, H. *Superlattices Microstruct.* **1997**, *21*, 259.

(19) Petroff, P. M. *NATO ASI Ser. E* **1995**, *298*, 49.

(20) Sopanen, M.; Lipsanen, H.; Ahopelto, J. *Appl. Phys. Lett.* **1995**, *67*, 3768.

(21) Carlsson, N.; Seifert, W.; Petersson, A.; Castrilo, P.; Pistol, M. E.; Samuelson, L. *Appl. Phys. Lett.* **1994**, *65*, 3093.

(22) Collier, C. P.; Saykally, R. J.; Shiang, J. J.; Henrichs, S. E.; Heath, J. R. *Science* **1997**, *277*, 1978.

(23) Takagahara, T. *Optoelectron.* **1993**, *8*, 545.

(24) Kagan, C. R.; Murray, C. B.; Nirmal, M.; Bawendi, M. G. *Phys. Rev. Lett.* **1996**, *76*, 1517; **1996**, *76*, 3043 (erratum).

(25) Kagan, C. R.; Murray, C. B.; Bawendi, M. G. *Phys. Rev. B* **1996**, *54*, 8633.

(26) Stafford, C. A.; S., D. S. *Phys. Rev. Lett.* **1994**, *72*, 3590.

(27) Ledentsov, N. N.; Grundmann, M.; Kirstaedter, N.; Schmidt, O.; Heitz, R.; Bohrer, J.; Bimberg, D.; Ustinov, V. M.; Shchukin, V. A.; Egorov, A. Y.; Zhukov, A. E.; Zaitsev, S.; Kop'ev, P. S.; Alferov, Z. I.; Ruvimov, S. S.; Kosogov, A. O.; Werner, P.; Gosele, U.; Heydenreich, J. *Solid-State Electron.* **1996**, *40*, 785.

(28) Ledentsov, N. N.; Boehrer, J.; Bimberg, D.; Zaitsev, S. V.; Ustinov, V. M.; Egorov, A. Y.; Zhukov, A. E.; Maximov, M. V.; Kopev, P. S.; et al. *Mater. Res. Soc. Symp.* **1996**.

(29) Nachtwei, G.; Liu, Z. H.; Kaya, I. I.; Luetjering, G.; Weiss, D.; Von Klitzing, K.; Eberl, K. *Phys.* Stat. *Solidi B* **1997**, *204*, 329.

(30) Aers, G. C.; Liu, H. C. *Solid State Commun.* **1990**, *73*, 19.

(31) Banin, U.; Cerullo, G.; Guzelian, A. A.; Bardeen, C. J.; Alivisatos, A. P.; Shank, C. V. *Phys. Rev. B* **1997**, *55*, 7059.

(32) Guzelian, A. A.; Katari, J. E. B.; Kadavanich, A. V.; Banin, U.; Hamad, K.; Juban, E.; Alivisatos, A. P.; Wolters, R. H.; Arnold, C. C.; Heath, J. R. *J. Phys. Chem.* **1996**, *100*, 7212.

(33) Micic, O. I.; Curtis, C. J.; Jones, K. M.; Sprague, J. R.; Nozik, A. J. *J. Phys. Chem.* **1994**, *98*, 4966.

(34) Micic, O. I.; Sprague, J. R.; Curtis, C. J.; Jones, K. M.; Machol, J. L.; Nozik, A. J. *J. Phys. Chem.* **1995**, *99*, 7754.

(35) Micic, O. I.; Sprague, J. R.; Lu, Z.; Nozik, A. J. *Appl. Phys. Lett* **1996**, *68*, 3150.

(36) Micic, O. I.; Cheong, H. M.; Fu, H.; Zunger, A.; Sprague, J. R.; Mascarenhas, A.; Nozik, A. J. *J. Phys. Chem. B.* **1997**, *101*, 4904.

(37) Fu, H.; Zunger, A. *Phys. Rev. B* **1997**, *56*, 1496.

(38) Fu, H.; Zunger, A. *Phys. Rev. B* **1997**, *55*, 1642.

(39) Efros, A. L.; Rosen, M. 1998. Manuscript to be published.

(40) Takagahara, T. *Surf. Sci.* **1992**, *267*, 310.

(41) Yoffe, A. D. *Adv. Phys.* **1993**, *42*, 173.

(42) Kagan, C. R. The Electronic and Optical Properties of Close Packed CdSe Quantum Dot Solids. Thesis, Massachusetts Institute of Technology, 1996.

(43) Cleveland, C. L.; Landman, U.; Schaaff, T. G.; Shafigullin, M. N.; Stephens, P. W.; Whetten, R. L. *Phys. Rev. Lett.* **1997**, *79*, 1873.

(44) Schaaff, T. G.; Shafigullin, M. N.; Khoury, J. T.; Vezmar, I.; Whetten, R. L.; Cullen, W. G.; First, P. N.; Wing, C.; Ascensio, J.; Yacaman, M. J. *J. Phys. Chem. B* **1997**, *101*, 7885.

(45) Harfenist, S. A.; Wang, Z. L.; Whetten, R. L.; Vezmar, I.; Alvarez, M. M. *Adv. Mater.* **1997**, *9*, 817.

(46) Zhang, B. P.; Wang, W. X.; Yasuda, T.; Segawa, Y.; Edamatsu, K.; Itoh, T. *Appl. Phys. Lett.* **1997**, *71*, 3370.

(47) Tang, Y. S.; Cai, S.; Jin, G.; Duan, J.; Wang, K. L.; Soyez, H. M.; Dunn, B. S. *Appl. Phys. Lett.* **1997**, *71*, 2448.

(48) Medeiros-Ribeiro, G.; Garcia, J. M.; Petroff, P. M. *Phys. Rev. B: Condens. Matter* **1997**, *56*, 3609.

(49) Chun, Y. J.; Nakajima, S.; Kawabe, M. *Jpn. J. Appl. Phys., Part 2* **1996**, *35*, L1075.

(50) Heath, J. R.; Williams, R. S.; Shiang, J. J.; Wind, S. J.; Chu, J.; D'Emic, C.; Chen, W.; Stanis, C. L.; Bucchignano, J. J. *J. Phys. Chem.* **1996**, *100*, 3144.

(51) Murray, C. B.; Norris, D. J.; Bawendi, M. G. *J. Am. Chem. Soc.* **1993**, *115*, 8706.

(52) Gu, Y.; Lin, Z.; Smetkowski, V.; Butera, R.; Waldeck, D. H. *Langmuir* **1995**, *11*, 1849.

(53) Wu, Y.; Micic, O. I.; Nozik, A. J. Unpublished results.

(54) Heller, A.; Aharon-Shalom, A.; Bonner, W. A.; Miller, B. *J. Am. Chem. Soc.* **1982**, *104*, 6942.

(55) Blanton, S. A.; Leheny, R. L.; Hines, M. A.; Guyot-Sionnest, P. *Phys. Rev. Lett.* **1997**, *79*, 865.

(56) Colvin, V. L.; Cunningham, K. L.; Alivisatos, A. P. *J. Chem. Phys.* **1994**, *101*, 7122.

(57) Guyot-Sionnest, P.; Micic, O. I.; Nozik, A. J. Unpublished results.

(58) Zaban, A.; Micic, O. I.; Gregg, B. A.; Nozik, A. J. *Langmuir* **1998**, *14*, 3153.